A study on the evolution of dielectric function of ZnO thin films with decreasing film thickness

Li, X. D.; Chen, T. P.; Liu, P.; Liu, Y.; Liu, Z.; Leong, K. C.

2014

Li, X. D., Chen, T. P., Liu, P., Liu, Y., Liu, Z., & Leong, K. C. (2014). A study on the evolution of dielectric function of ZnO thin films with decreasing film thickness. Journal of Applied Physics, 115(10), 103512-.

https://hdl.handle.net/10356/104196

https://doi.org/10.1063/1.4868338

A study on the evolution of dielectric function of ZnO thin films with decreasing film thickness

X. D. Li, T. P. Chen, P. Liu, Y. Liu, Z. Liu, and K. C. Leong

Citation: Journal of Applied Physics **115**, 103512 (2014); doi: 10.1063/1.4868338
View online: http://dx.doi.org/10.1063/1.4868338
View Table of Contents: http://scitation.aip.org/content/aip/journal/jap/115/10?ver=pdfcov
Published by the AIP Publishing

A study on the evolution of dielectric function of ZnO thin films with decreasing film thickness

X. D. Li,[1] T. P. Chen,[1,a)] P. Liu,[1] Y. Liu,[2] Z. Liu,[3] and K. C. Leong[4]
[1]*School of Electrical and Electronic Engineering, Nanyang Technological University, 639798 Singapore*
[2]*State Key Laboratory of Electronic Thin Films and Integrated Devices, University of Electronic Science and Technology, Chengdu 610054, People's Republic of China*
[3]*School of Materials and Energy, Guangdong University of Technology, Guangzhou 510006, People's Republic of China*
[4]*GLOBALFOUNDRIES Singapore Pte Ltd, 738406 Singapore*

(Received 11 October 2013; accepted 2 March 2014; published online 12 March 2014)

Dielectric function, band gap, and exciton binding energies of ultrathin ZnO films as a function of film thickness have been obtained with spectroscopic ellipsometry. As the film thickness decreases, both real (ε_1) and imaginary (ε_2) parts of the dielectric function decrease significantly, and ε_2 shows a blue shift. The film thickness dependence of the dielectric function is shown related to the changes in the interband absorption, discrete-exciton absorption, and continuum-exciton absorption, which can be attributed to the quantum confinement effect on both the band gap and exciton binding energies. © *2014 AIP Publishing LLC*. [http://dx.doi.org/10.1063/1.4868338]

I. INTRODUCTION

In recent years, zinc oxide (ZnO), which is a transparent oxide semiconductor with a wide band gap of ~3.4 eV and a large exciton binding energy of ~60 meV, has been intensively studied due to its promising applications in optoelectronics.[1,2] When ZnO films and associated devices are scaled down to nanoscale regime, due to the quantum confinement effect, the nanoscale structures exhibit some unique properties different from their bulk counterparts. The size dependence, which provides us the possibility to tune the material properties, is of great interest to be studied. In our previous work, it has been revealed that the quantum confinement effect has a significant impact on the optical properties of ultrathin ZnO and Al-doped ZnO films, in particular, the excitonic absorption near the absorption band edge.[3] On the other hand, it was reported that quantum confinement effect has a significant influence on the dielectric functions of the Si and Ge nanocrystals embedded in a SiO_2 matrix, e.g., the magnitude of the dielectric functions is reduced with decreasing nanocrystal size.[4,5] Therefore, it would be interesting to examine the film-thickness dependence of the complex dielectric function of the ultrathin ZnO films as quantum confinement effect could play an important role in such system.

In this work, the complex dielectric function of ultrathin ZnO films as a function of the film thickness has been investigated with spectroscopic ellipsometry (SE). It is observed that the complex dielectric function is strongly dependent of the film thickness, e.g., the magnitudes of both real and imaginary parts of the complex dielectric function decrease with decreasing film thickness and are significantly smaller than that of bulk ZnO. It is shown that the phenomenon can be attributed to the quantum confinement effect on both the band gap and exciton binding energies of the ZnO thin films.

II. EXPERIMENT

ZnO thin films with various thicknesses were deposited onto a 30 nm SiO_2 buffer layer which was thermally grown on a HF-cleaned *p*-type Si wafer by dry oxidation. The oxide buffer layer was used to minimize the substrate-induced stress effect[6] and provide a film configuration (ZnO/SiO_2) that is similar to the one (ZnO thin film/quartz substrate) used in the optical absorbance measurement. The ZnO deposition was carried out by RF magnetron sputtering using a pure ZnO target (99.99% in purity). The sputtering was conducted with a RF power of 80 W at room temperature in argon ambient with a background pressure of 9×10^{-3} Torr (the base pressure was 7×10^{-6} Torr). The pure argon environment was to ensure that the influence of oxygen on the structural and optical properties of the deposited films is minimized.[7,8] The crystalline structures of the ZnO thin films were characterized by X-ray diffraction (XRD) (Siemens D5005) in θ-2θ geometry using Cu Kα radiation (40 kV, 40 mA). The XRD analysis indicates the polycrystalline growth of the ZnO films with the wurtzite structure along [002] orientation. The film surface morphology was investigated using scanning electron microscope (SEM) (LEO 1550 Gemini). The average grain sizes of the ZnO thin films estimated from the XRD measurement are comparable with that from the SEM measurement; and both measurements indicate that the average grain size increases with increasing film thickness. The situation is similar to that reported in our previous study.[3] Spectroscopic ellipsometric (SE) measurement was carried out with an ellipsometer (Woollam VB-250) in the wavelength range of 250-1100 nm with a step size of 5 nm at the three incident angles of 65°, 70°, and 75°, respectively. The thickness values obtained

a)Author to whom correspondence should be addressed. Electronic mail: echentp@ntu.edu.sg

from the SE fittings for the various films are very close to the nominal values of 10, 20, 40, 90, and 185 nm, respectively. Optical absorbance measurement was carried out with an UV-Vis spectrophotometer (Perkin-Elmer 950) on the samples of ZnO thin films deposited on quartz substrate in the wavelength range of 250–800 nm.

III. MODELING AND SE SPECTRAL FITTING

The SE analysis is based on the five-phase model (i.e., air/surface-roughness layer/ZnO layer/SiO_2 buffer layer/Si substrate) shown in the inset of Fig. 1(a). The surface-roughness layer is modeled with an effective layer consisting of air voids and ZnO based on the Bruggeman effective medium approximation (EMA),[9]

$$\frac{\varepsilon_{ZnO}-\varepsilon_i}{\varepsilon_{ZnO}+2\varepsilon_i}f+\frac{\varepsilon_{air}-\varepsilon_i}{\varepsilon_{air}+2\varepsilon_i}(1-f)=0, \tag{1}$$

where ε_i is the effective complex dielectric function of the surface-roughness layer, f is the volume fraction of ZnO in the surface-roughness layer, ε_{air} is the dielectric constant of air void ($\varepsilon_{air}=1$ assumed in all SE analysis), and $\varepsilon_{ZnO}(=\varepsilon_1+i\varepsilon_2$, where ε_1 and ε_2 are the real part and imaginary part of the complex dielectric function) is the complex dielectric function of ZnO. Here, ε_{ZnO} is the parameter to be determined from the SE analysis. Detail of the modeling and determination of ε_{ZnO} is discussed below.

Dielectric function of bulk ZnO films has been intensively studied based on various models such as the Forouhi-Bloomer (F-B) model,[10] the Tauc-Lorentz (T-L) model,[11] and Holden's model.[12,13] It has been known that the presence of excitons near the band edge significantly influences the dielectric function in the energy range.[14] The formation of excitons are attributed to the three valence bands of wurtzite ZnO, labeled in order of the valence bands as "A", "B," and "C".[15] The three excitons usually merge into a broadened peak at room temperature due to the broadening caused by the exciton-phonon interactions.[16] In this work, the dielectric function of the ZnO thin films is determined based on the model proposed by Yoshikawa and Adachi,[17]

$$\varepsilon(E)=\varepsilon_\infty+\varepsilon_{\text{int}}(E)+\varepsilon_d(E)+\varepsilon_c(E), \tag{2}$$

where ε_∞ is the high frequency dielectric constant, $\varepsilon_{\text{int}}(E)$ is the complex dielectric function due to the interband absorption, and $\varepsilon_d(E)$ and $\varepsilon_c(E)$ are the complex dielectric function due to the discrete and continuum excitonic absorptions, respectively. The interband absorption is modeled with a simplified critical point model at E_0 transition. $\varepsilon_{\text{int}}(E)$ due to the three valence bands A, B, C is described with[17]

$$\varepsilon_{\text{int}}(E)=\sum_{\alpha=A,B,C}A_{0\alpha}^{\text{int}}E_{g\alpha}^{-1.5}f(\chi_{0\alpha}), \tag{3}$$

where $f(\chi_{0\alpha})=\chi_{0\alpha}^{-2}[2-(1+\chi_{0\alpha})^{1/2}-(1-\chi_{0\alpha})^{1/2}]$,

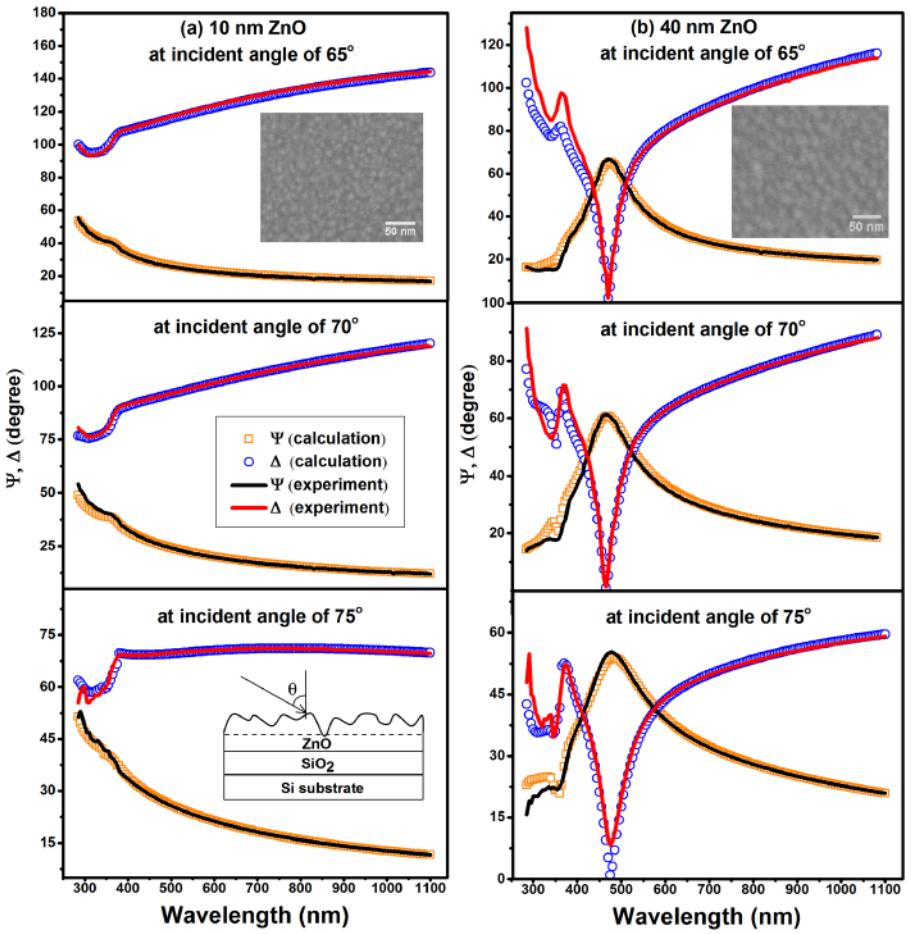

FIG. 1. SE spectral fittings of the 10 nm (a) and 40 nm (b) ZnO thin films deposited on the SiO_2 buffer layer for three different incident angles. SEM images of the thin films are shown in the figure. The five-phase model used in the SE modeling is shown in the inset of (a) also.

$$\chi_{0\alpha} = (E + i\Gamma_{0\alpha}^{\text{int}})/E_{g\alpha},$$

where $A_{0\alpha}^{\text{int}}$ is the interband strength parameter, $\Gamma_{0\alpha}^{\text{int}}$ is the broadening parameter, $E_{g\alpha}$ is the band gap energy corresponding to the E_0 gaps at three valence bands A, B, and C. $\varepsilon_d(E)$ is modeled with a broadened Lorentzian line shape[18]

$$\varepsilon_d(E) = \sum_{\alpha=A,B,C}\left[\sum_{n=1}^{\infty}\frac{A_{0\alpha}^{d}}{n^3}\frac{1}{E_{g\alpha}-\frac{R_\alpha}{n^2}-E-i\Gamma_{n,\alpha}^{d}}\right], \quad (4)$$

where $A_{0\alpha}^{d}$ is the discrete-exciton strength parameter, R_α is the exciton binding energy, $\Gamma_{n,\alpha}^{d}$ is the broadening parameter of the nth discrete state (since the intensity falls with n^{-3}, only the ground state $n=1$ is considered in this work). $\varepsilon_c(E)$ is described by[17]

$$\varepsilon_c(E) = \sum_{\alpha=A,B,C}\frac{A_{0\alpha}^{c}(E_{g\alpha}-R_\alpha)}{4R_\alpha(E+i\Gamma_\alpha^{c})^2}\cdot\ln\frac{(E_{g\alpha})^2}{(E_{g\alpha})^2-(E+i\Gamma_\alpha^{c})^2}, \quad (5)$$

where $A_{0\alpha}^{c}$ is the continuum-exciton strength parameter. Γ_α^{c} is the broadening parameter.

The ellipsometric angles (Ψ and Δ) are functions of wavelength, thicknesses d_s, d_{ZnO}, and d_{SiO_2} of the surface-roughness layer, ZnO layer and SiO_2 buffer layer, respectively, volume fraction f of ZnO in the surface-roughness layer, and dielectric functions of SiO_2, bulk Si and ZnO thin films. In the calculations of Ψ and Δ, the complex dielectric functions of both SiO_2 and bulk Si from Ref. 19 were used; and Eqs. (2)–(5) were used to calculate the complex dielectric function of the ZnO thin films. As there were large fluctuations in the experimental data for wavelengths shorter than 285 nm due to the high noise level in short wavelengths, the spectral fitting was carried out in the wavelength range of 285–1100 nm by freely varying the parameters ($A_{0\alpha}^{\text{int}}$, $\Gamma_{0\alpha}^{\text{int}}$, $A_{0\alpha}^{d}$, $\Gamma_{n,\alpha}^{d}$, $A_{0\alpha}^{c}$, Γ_α^{c}, $E_{g\alpha}$, R_α, d_s, d_{ZnO}, d_{SiO2}, f) to minimize the mean-squared-error of the comparison between the calculated and experimentally measured Ψ and Δ.[20] Excellent fittings with goodness of fit $\chi^2 < 20$ were achieved for all the film thicknesses. As examples, Figure 1 shows the SE spectral fittings of the ZnO thin films with the thicknesses of 10 and 40 nm. By using the values of the parameters of Eqs. (2)–(5) yielded from the spectral fittings in the wavelength range of 285–1100 nm, we calculated the real part (ε_1) and imaginary part (ε_2) of the complex dielectric function of the ZnO films with Eqs. (2)–(5) in the extended photon energy range of ~1.1–~5 eV (i.e., the wavelength range of 250–1100 nm). The calculated ε_1 and ε_2 of the ZnO thin films with various thicknesses are shown in Fig. 2. With the ε_1 and ε_2 values, we were also able to calculate the absorption coefficient α (Ref. 21) of the ZnO thin films in the photon energy range of ~1.1–~5 eV. Figure 3 shows the comparison between the calculated and measured α for the ZnO thin film with the thickness of ~20 nm. Note that the normalized value of the absorption coefficient instead of the absolute value is used in the figure. This is to eliminate the effect of some difference in the film thickness between the sample used in the SE analysis and the one used in the absorbance measurement. As can be observed in the figure, the calculation generally agrees well with the experimental result (note that there is a small departure for photon energies lower than ~3 eV, which could be due to the fact that defect absorption is not included in the modeling). This indicates that the models used in the SE analysis are accurate and the above approach is reliable.

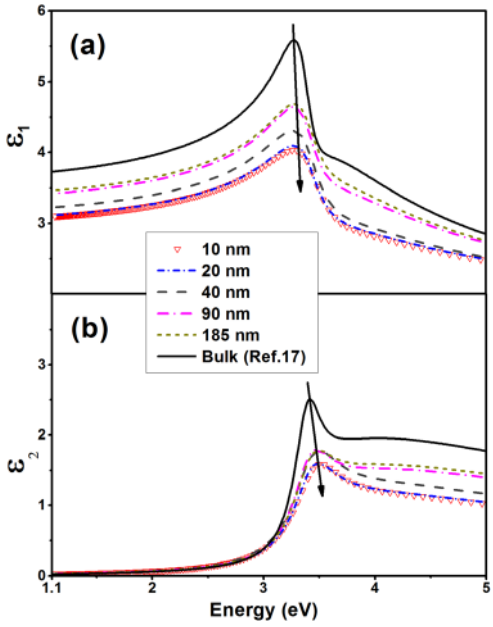

FIG. 2. (a) Real part (ε_1) and (b) imaginary part (ε_2) of the complex dielectric function of the ZnO thin films with various thicknesses obtained from the spectral fittings. The bulk value (Ref. 17) is included for comparison.

IV. DISCUSSIONS

As can be observed in Fig. 2, the film thickness has a significant impact on the dielectric function of ZnO thin films. As compared to the bulk counterpart,[17] the ultrathin ZnO films exhibit a significant reduction in the magnitudes of both real and imaginary parts of the complex dielectric function, which can be attributed to the quantum confinement effect. The quantum confinement effect could be mainly related to the small sizes (a few nanometers) of the

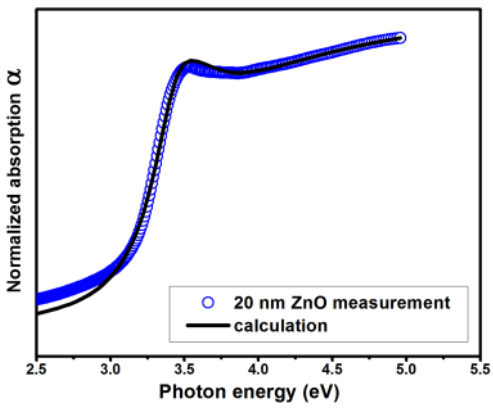

FIG. 3. Comparison of the normalized absorption coefficient of ZnO thin film with the thickness of 20 nm between the calculation using the ε_1 and ε_2 values obtained from the SE spectral fitting and the absorbance measurement.

grains in ZnO thin films. The reduction is found more significant in a thinner film due to the stronger confinement in a smaller grain, e.g., as compared to bulk ZnO, the ZnO thin film with the thickness of 20 nm (average grain size $D = 6.8$ nm) shows a significant reduction of ~26% and ~37% in the real and imaginary parts of the complex dielectric function at the photon energy of 3.3 eV, respectively, while the ZnO thin film with the thickness of 90 nm (average grain size $D = 15.5$ nm) only shows a reduction of ~16% and ~29%, respectively. The peaks also show a small blue shift with reduction in the film thickness.

Figure 4 shows the exciton binding energies and band gap energy of the ZnO thin films obtained from the SE spectral fittings as a function of average grain size. As shown in the figure, a strong quantum size effect can be observed. Both the exciton binding energies and band gap energy increase with decreasing grain size. Band gap expansion due to quantum confinement is a well-known phenomenon.[5,16] The increase in exciton binding energies is due to the confinement of electron-hole wave function in the small dimensions.[22] The confinement enhances the columbic interaction of an exciton, giving rise to an increase in the exciton binding energy.[23] As shown in Figs. 4(a) and 4(b), the size dependence of average exciton binding energies and band gap energy could be roughly described by the trend lines of $R_{AV}(\text{meV}) = 60 + 926/D(\text{nm})^{1.62}$ and $E_g(\text{eV}) = 3.46 + 3.23/D(\text{nm})^{1.65}$, respectively. These results are consistent with our previous absorption study,[3] which is shown in the insets of Fig. 4. On the other hand, it is also worthy to point out that in addition to the confinement in the nanocrystals, one-dimension confinement (i.e., the confinement in the thickness direction) in a continuous thin film may also play a role.

In a confined nanostructure, the reduction of optical constant or dielectric function is typically associated with the band gap opening.[24] In a classic description, the reduction of dielectric function could be explained by the reduction of electron polarization induced by the distortion of electrons in the atoms as the result of the band gap expansion; while quantum mechanically, it could be explained by the increase of the band gap energy, which makes it more difficult for electrons to transit from the valance band to the conduction band. Figure 5 shows the contributions of the interband absorption ($\varepsilon_{\text{int},imag}$), discrete-exciton absorption ($\varepsilon_{d,imag}$), and continuum-exciton absorption ($\varepsilon_{c,imag}$) to the imaginary part (ε_2) of the complex dielectric functions of the ZnO thin films with the thicknesses of 20 and 90 nm. The corresponding counterparts of bulk ZnO (Ref. 17) are also included for comparison. As can be observed in the figure, all the absorptions ($\varepsilon_{\text{int},imag}$, $\varepsilon_{d,imag}$, and $\varepsilon_{c,imag}$) exhibit a film-thickness dependence, i.e., they are smaller and show a blue shift for a thinner film, which is responsible for the film-thickness dependence of dielectric function shown in Fig. 2. It is noticed from Fig. 5 that $\varepsilon_{\text{int},imag}$ and $\varepsilon_{c,imag}$ have a more significant film-thickness dependence than $\varepsilon_{d,imag}$. It has been known that the continuum excitonic absorption will become proportional to $(E - E_g)^{1/2}$ when $E \gg E_g$, in the form similar to the interband absorption above the E_g.[25] Therefore, for a thinner ZnO film, with the band gap expansion as a result of quantum confinement effect, both the interband absorption ($\varepsilon_{\text{int},imag}$) and continuum-exciton absorption ($\varepsilon_{c,imag}$) decrease. It can be also understood that increase in the transition energy makes the transition more difficult resulting in reduction in the polarizability. It can be concluded that the reduction in ε_2 is mainly due to the reduction in both the interband absorption ($\varepsilon_{\text{int},imag}$) and continuum-exciton absorption ($\varepsilon_{c,imag}$). For the contribution of the discrete-exciton absorption ($\varepsilon_{d,imag}$), the situation is more complicated. As shown in Fig. 5(b), as compared to

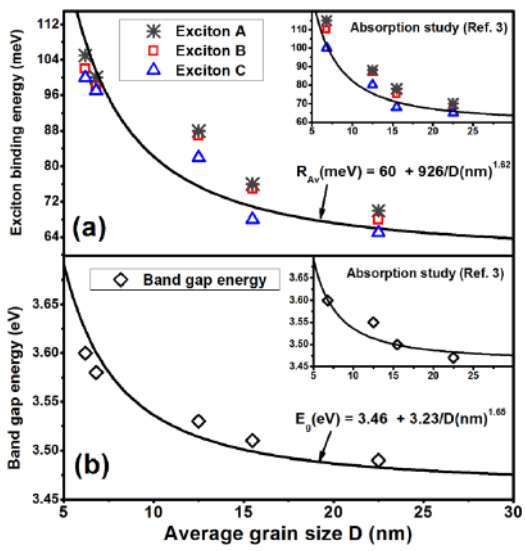

FIG. 4. (a) Exciton binding energies and (b) band gap energy of the ZnO thin films obtained from the SE analysis as a function of the average grain size D (D is determined from the SEM images). The insets show the same size dependence of exciton binding energies and band gap energy of the ZnO thin film obtained from an absorption study (Ref. 3). The trend lines of the size dependence are for guiding the eyes only.

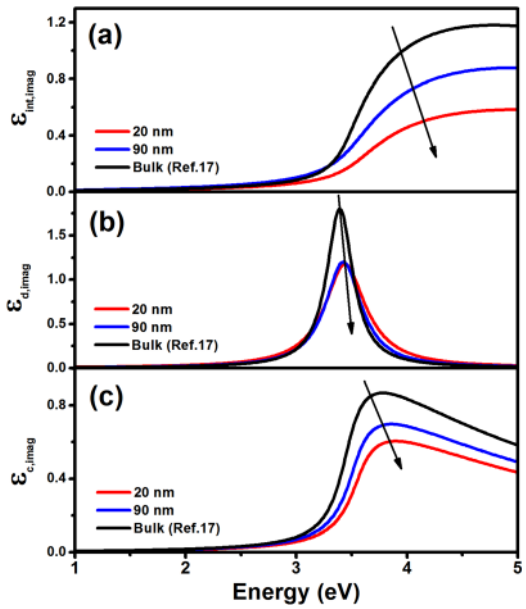

FIG. 5. Contributions of the interband absorption ($\varepsilon_{\text{int},imag}$) (a), discrete-exciton absorption ($\varepsilon_{d,imag}$) (b) and continuum-exciton absorption ($\varepsilon_{c,imag}$) (c) to the imaginary part (ε_2) of the complex dielectric function of the ZnO thin films with the thicknesses of 20 and 90 nm. The bulk values (Ref. 17) are included for comparison.

the bulk counterpart, both the 20 and 90 nm ZnO thin films exhibit a reduction in the oscillator strength of the discrete-exciton absorption. However, the reduction of the 20 nm sample is not more significant than that of the 90 nm sample. This is because increase in the exciton binding energy (see Fig. 4(a)) due to quantum confinement effect results in stabilization of the exciton.[26]

V. CONCLUSIONS

The complex dielectric function, band gap energy, and exciton binding energies of ultrathin ZnO films deposited by RF magnetron sputtering have been obtained from the SE analysis based on the Yoshikawa and Adachi's model. As compared to bulk ZnO, the ultrathin films exhibit a significant reduction in both real and imaginary parts of the dielectric function, accompanied by the increase in both band gap energy and exciton binding energies. The reduction in the complex dielectric function is mainly attributed to the reduction in the interband absorption and continuum-exciton absorption due to the band gap expansion induced by the quantum confinement effect, while discrete-exciton absorption is not significantly reduced due to the increase in the exciton binding energy, which is also the consequence of the confinement effect.

ACKNOWLEDGMENTS

This work was financially supported by MOE Tier 1 Grant (Grant No. RG 43/12) and the Si COE Program. Y. Liu would like to acknowledge the support by NSFC under Project No. 61274086.

[1]S. J. Pearton, D. P. Norton, K. Ip, Y. W. Heo, and T. Steiner, Prog. Mater. Sci. **50**, 293 (2005).
[2]U. Ozgur, Y. I. Alivov, C. Liu, A. Teke, M. A. Reshchikov, S. Dogan, V. Avrutin, S.-J. Cho, and H. Morkoc, J. Appl. Phys. **98**, 041301 (2005).
[3]X. D. Li, T. P. Chen, P. Liu, Y. Liu, and K. C. Leong, Opt. Express **21**, 14131 (2013).
[4]T. P. Chen, Y. Liu, M. S. Tse, O. K. Tan, P. F. Ho, K. Y. Liu, D. Gui, and A. L. K. Tan, Phys. Rev. B **68**, 153301 (2003).
[5]E. S. M. Goh, T. P. Chen, S. F. Huang, Y. C. Liu, and C. Q. Sun, J. Appl. Phys. **109**, 064307 (2011).
[6]R. Ghosh, D. Basak, and S. Fujihara, J. Appl. Phys. **96**, 2689 (2004).
[7]S. Kishimoto, T. Yamada, K. Ikeda, H. Makino, and T. Yamamoto, Surf. Coat. Technol. **201**, 4000 (2006).
[8]S. S. Kim and B.-T. Lee, Thin Solid Films **446**, 307 (2004).
[9]D. A. G. Bruggeman, Ann. Phys. **416**, 636–664 (1935).
[10]L. Miao, S. Tanemura, M. Tanemura, S. P. Lau, and B. K. Tay, J. Mater. Sci.: Mater. Electron. **18**, S343 (2007).
[11]H. Fujiwara and M. Kondo, Phys. Rev. B **71**, 75109 (2005).
[12]K. Postava, H. Sueki, M. Aoyama, T. Yamaguchi, and C. Ino, J. Appl. Phys. **87**, 7820 (2000).
[13]G. E. Jellison, Jr. and L. A. Boatner, Phys. Rev. B **58**, 3586 (1998).
[14]T. Holden, P. Ram, F. H. Pollak, J. L. Freeouf, B. X. Yang, and M. C. Tamargo, Phys. Rev. B. **56**, 4037 (1997).
[15]S. Adachi, *Optical Properties of Crystalline and Amorphous Semiconductors: Materials and Fundamental Principles* (Kluwer Academic Publishers, 1999), Chap. 1.
[16]J. C. Nie, J. Y. Yang, Y. Piao, H. Li, Y. Sun, Q. M. Xue, C. M. Xiong, R. F. Dou, and Q. Y. Tu, Appl. Phys. Lett. **93**, 173104 (2008).
[17]H. Yoshikawa and S. Adachi, Jpn. J. Appl. Phys. Part 1 **36**, 6237 (1997).
[18]S. Ninomiya and S. Adachi, J. Appl. Phys. **78**, 4681 (1995).
[19]E. D. Palik and G. Ghosh, *Handbook of Optical Constants of Solids* (Academic Press, 1998).
[20]R. M. A. Azzam and N. M. Bashara, *Ellipsometry and Polarized Light* (North-Holland, 1977), Chap. 3.
[21]M. Fox, *Optical Properties of Solids* (Oxford, 2001), Chap. 1.
[22]R. Fausto, G. Guido, M. Oskar, and M. Elisa, J. Phys.: Condens. Matter **11**, 5969 (1999).
[23]H. Gotoh and H. Ando, J. Appl. Phys. **82**, 1667 (1997).
[24]L.-W. Wang and A. Zunger, Phys. Rev. Lett. **73**, 1039 (1994).
[25]R. J. Elliott, Phys. Rev. **108**, 1384 (1957).
[26]G. T. Einevoll, Phys. Rev. B **45**, 3410 (1992).